IEEE Access
Multidisciplinary | Rapid Review | Open Access Journal

Received November 9, 2021, accepted January 5, 2022, date of publication January 11, 2022, date of current version January 20, 2022.

Digital Object Identifier 10.1109/ACCESS.2022.3142114

PN Code Acquisition in DS-CDMA Wireless Systems Using Smart Antenna and S-CFAR Processor

TAGHREED SAAD ALOFAISAN[1], AMR M. RAGHEB[2], AHMED B. IBRAHIM[2], MUSAED ALHUSSEIN[1], AND SALEH A. ALSHEBEILI[2]

[1]Computer Engineering Department, King Saud University, Riyadh 11421, Saudi Arabia
[2]Electrical Engineering Department, King Saud University, Riyadh 11421, Saudi Arabia

Corresponding author: Taghreed Saad Alofaisan (talofaisan.c@ksu.edu.sa)

This work was supported by the Researchers Supporting Project, King Saud University, Riyadh, Saudi Arabia, under Grant RSP-2021/46.

ABSTRACT Code division multiple access (CDMA) is a class of techniques allowing multiple users to transmit simultaneously to meet the demand of the recently unprecedented revolution in wireless services. In CDMA systems, a unique pseudo-random (PN) code is assigned to each user to spread the signal at the transmitter side and facilitate signal's recovery at the receiver side. In particular, a CDMA receiver initially seeks synchronization or acquisition of PN code. This paper focuses on the development and analysis of a new adaptive serial search acquisition method for direct sequence (DS)-CDMA systems in Rayleigh slowly fading channels. The proposed method makes use of smart antenna and switched constant false alarm (S-CFAR) processor for PN code acquisition. The smart antenna and S-CFAR processor are employed to improve the PN acquisition performance by adjusting a decision threshold according to the environment. The performance of proposed acquisition system has been evaluated in terms of probability of false alarm, probability of detection, and mean acquisition time. Closed form expressions for the probability of false alarm and probability of detection have been derived. Further, numerical and simulation results have been presented to show the performance of proposed PN acquisition system in comparison with other existing CFAR-based PN acquisition schemes.

INDEX TERMS PN acquisition, S-CFAR adaptive thresholding, smart antenna, direct sequence CDMA, mobile communication.

I. INTRODUCTION

This decade is witnessing an unprecedented revolution in the field of wireless communications. A main motivation deriving the new developments in wireless technology is to allow the user access to a broad spectrum of services offered by the global communication network with cost effectiveness, high date rates, high reliability, and less latency, at any time and without regard to location or mobility [1], [2]. The demand for wireless services has exceeded expectations in recent years. This is evident from the annual spending of global telecom services, which is anticipated to be 1.575 billion US dollars for the year 2021 [3].

A major issue of concern in the design of digital communication is to provide efficient utilization of power and bandwidth. Nevertheless, there are situations where it is necessary to sacrifice the efficient utilization of these two parameters in order to meet certain other design objectives [4]. An example of such situations is in the spread spectrum (SS) communication where the transmission bandwidth is greater than the message bandwidth. For instance, an SS system distributes a baseband signal, having a bandwidth of only few kilohertz, over a bandwidth that may occupy megahertz range.

SS systems have been used in both military and commercial communications. In military communications, SS was used to prevent eavesdropping and to overcome intentional jamming. However, for commercial applications, SS multiple access communication has been extensively used building

The associate editor coordinating the review of this manuscript and approving it for publication was Ali Kashif Bashir.

upon its advantage of combating un-intended noise due to the channel fading and intersymbol interference (ISI).

Code-division multiple-access (CDMA) is a scheme which makes use of a unique pseudonoise (PN) code to spread the message signal to a relatively wide bandwidth. The main motivation for spreading message bandwidth is to enhance processing gain, reduce interference, and differentiate between the users. Because CDMA is performed with no requirement for time or frequency division, the system's capacity gets enhanced.

In direct sequence (DS)-CDMA systems, PN code synchronization is first performed, where a replica of the PN code is cross-correlated with the received signal to recover the information signal. In particular, two phases are employed to perform time synchronization of the PN code embedded in the received signal and the local PN code generated at the receiver. First, initial synchronization or acquisition is conducted, where the two PN codes come into coarse alignment within one chip interval. Fine alignment and maintaining it are usually accomplished via a code-tracking loop.

Serial and parallel search methods have generally been considered for code acquisition. Serial search schemes test each possible uncertainty code phase in a sequential manner, while parallel search adopts the strategy of simultaneous testing all or part of possible code phases [5], [6]. Hybrid search methods were also considered, which combine both serial and parallel search methods [7], [8].

PN acquisition can be viewed as a classical binary testing problem with two hypotheses: H_1 hypothesis for correct code phase that results in the synchronization (alignment) state, and H_0 hypothesis for incorrect code phase that results in the non-synchronization (non-alignment) state. A threshold is usually stored at the receiver to determine if the two PN sequences are in alignment. This threshold is compared with the PN sequences' cross correlation value. If the correlation value exceeds the threshold, a decision is made in favor of H_1. Otherwise, it is set in favor of H_0. Note that errors can be made by the PN acquisition loop, leading to a false alarm or a miss. The former case occurs when the cross correlation value of two non-aligned PN sequences exceeds the stored threshold, while the second case occurs when the cross correlation value of two aligned PN sequences is below the stored threshold. Therefore, proper setting of threshold value is of paramount importance, as it may seriously degrade system performance especially in time-varying environments. In the following subsection, we present a brief review for the relevant works pertaining to the solutions proposed for such an important problem.

A. RELATED WORK

The most proposed scheme in the literature to align the received SS signal with the spreading signal generated locally is the serial PN code acquisition [5], [6]. This is due to the complexity, size, and cost of the parallel and hybrid acquisition techniques. Several methods have addressed the serial PN acquisition in a single-antenna DS-CDMA system operating with fixed or adaptive detection threshold; e.g., [9]–[12]. However, DS-CDMA communication systems employing multiple (array of) antennas for both transmission and/or reception have been considered. In such systems, the received signals from each antenna are combined in a proper signal processing setting to improve the statistics of the detector, and consequently the PN acquisition [13]. The antenna elements are often arranged with enough distance between them to ensure diversity, allowing the corresponding antenna channels have independent fading processes. Closer inter-element separation (in the order of a half wavelength of operating frequency) results in smart antenna configuration where adaptive antenna with beamforming is employed [13].

PN code acquisition utilizing antenna diversity has been widely investigated in the literature [11], [13]–[17]. However, smart antenna has distinctive advantages in terms of reducing multipath fading, ability in combating multiple access interference (MAI), and tracking mobile signals, which made it the focus of several studies for improving PN code acquisition [18], [19]. In [10] and [18], PN code acquisition methods exploiting all smart antenna elements have been proposed. It has been demonstrated by simulations that the use of smart antenna system for PN acquisition improves the detection performance and the mean acquisition time compared to using just a single antenna for the acquisition under additive white Gaussian noise (AWGN) and Rayleigh fading channels.

Smart antenna systems employing constant false alarm rate (CFAR) processors for PN acquisition have found a fertile environment in DS-CDMA communication systems. These processors are originally developed for radar signal detection [20]. Generally CFAR processors work by serially sending the received samples into a finite length shift register. The middle element of shift register is called the cell under test. The contents of cells surrounding the cell under test, which is referred to as a reference window, are processed to form a statistic representing the power level estimate. Multiplying this statistic by a positive constant achieves a desired probability of false alarm. Building upon this notion, an adaptive order statistic (OS)-CFAR acquisition processor has been introduced in [21]. The OS-CFAR has an inherent immunity against multipath interference since its adaptive threshold is based on the k^{th} smallest sample in the reference window. The smart antenna with the censored mean level detector (CMLD)-CFAR and the trimmed mean (TM)-CFAR have been proposed in [22] and [23], respectively, for PN code acquisition. These processors implement ordering followed by arithmetic averaging after censoring a small number of largest values in the ordered reference window, due to the effects of multipath signals. The results showed that a considerable improvement in the detection probability in a Rayleigh slowly fading multipath channel can be achieved compared to the schemes based on fixed thresholding.

Automatic censoring of interfering samples of ordered reference window has been also proposed for CFAR-based PN acquisition [24]. In such a technique, the number of interfering samples is first estimated and then the interfering

samples are censored from the reference window before adaptive threshold computation.

B. PAPER CONTRIBUTIONS AND ORGANIZATION

In this paper, we develop and analyse a new adaptive PN code acquisition scheme for DS-CDMA systems, which are widely used in military and civilian mobile communications. Our development involves, for the first time in literature, the use of smart antenna and switched (S)-CFAR processor for adaptive PN code acquisition. The proposed acquisition scheme adopts the serial search strategy and is intended for Rayleigh fading channels. The S-CFAR processor, originally introduced in [25] and [26] for radar signal detection, differs from the previously mentioned CFAR processors, where it enjoys the following features:

- it exploits the cell under test to form two reference windows, from which the power of background noise is estimated.
- it is simple to implement as it does not need ordering of reference window samples.
- it has parameters that can be tuned to achieve a small CFAR loss for a homogeneous environment and to achieve an enhanced robustness in the presence of MAI.

The organization of this paper is as follows. Section II reviews the CFAR processors elementary concepts and gives details of S-CFAR processor. Section III introduces the smart antenna system model and derives the probability of detection (P_d) and probability of false alarm (P_{fa}) for the proposed adaptive PN acquisition scheme. Section IV is concerned with the performance evaluation of proposed acquisition scheme, where numerical and simulation results are presented and discussed. Section V presents concluding remarks.

II. ADAPTIVE CFAR DETECTION

This section aims at explaining the technical background pertaining to adaptive CFAR detection, which will be used in the next section for the development of new PN code acquisition method. First, radar principles and basic elements of adaptive CFAR detection are briefly described. Next, discussion is presented for some of the adaptive CFAR techniques that are widely used for radar target detection in the presence of Gaussian noise. The discussion is limited to those techniques, which have been used in PN code acquisition. The CFAR processor that is of our focus in this study is also presented.

A. PRELIMINARIES

The concept of CFAR processors was originally introduced in the literature of radars [20], whose main functions are the detection and location of objects (or targets) often in the presence of thermal noise and clutter [27]. The term ''clutter'' refers to any echo of undesired signal, possibly caused by clouds, buildings, the sea, etc., that are reflected back to the receiver. Such disturbances greatly affect the performance of the radar receiver, which is required to achieve maximum probability of target detection and constant false alarm rate. In the past, the received signal samples are compared with a predetermined fixed threshold. This threshold is set to achieve a specified P_{fa}. If the receiver output is greater than this threshold, then signal sample under processing is declared a target, otherwise it is declared noise only. In practice, the returned signal from a target has unknown variance at the receiver input. Therefore, noise alone might exceed low level thresholds, leading in such a case to a false alarm. In contrast, if the threshold was set too high, weak target echoes might not be detected; this later situation is classified as a miss detection.

For reliable target detection in noisy environment, the threshold must be varied adaptively to maintain a constant false alarm rate [20], [28]. In modern radar systems, an adaptive threshold based on a CFAR processor is used so that the detection decision is done automatically. Based on a desired P_{fa}, the detection threshold is dynamically determined by multiplying a positive constant with the estimate of local background noise/clutter power [29]. Figure 1 shows a general CFAR detection scheme with received samples fed serially into a shift register of length $N + 1$. The statistic Z, representing the estimate of total noise power, is formed by processing the contents of N reference samples surrounding the sample under investigation whose content is Y. If Y exceeds the threshold $T = \alpha Z$, then a target is declared to be present. Here α denotes a constant scale factor, which is set to achieve a desired constant P_{fa}, when the total background noise is homogeneous, for a given reference window of size N. The probability of achieving a homogeneous clutter sample within the reference window is greatly affected by the size N of the reference window. Next, we present a review of common CFAR techniques developed for radar target detection and later used for PN code acquisition in CDMA systems.

B. THE CELL AVERAGING (CA)- CFAR PROCESSOR

In CA-CFAR processors, the total noise power is estimated using arithmetic averaging of reference window samples. Good estimates of the noise power can be obtained by such processors under certain conditions. Specifically, the CA-CFAR processor is the optimum CFAR processor, which maximizes the detection probability at a constant P_{fa}, in a homogeneous background when the reference window contains independent and identically distributed (i.i.d) observations governed by an exponential distribution. However, significant degradation in the CA processor performance occurs in a non-homogeneous background. Non-homogeneity may occur due to the presence of interfering targets in the reference window. Next, we introduce the OS-CFAR scheme, which alleviates these problems to some degree [20], [30]–[32].

C. THE OS-CFAR PROCESSOR

Unlike, the CA-CFAR processor which makes use of arithmetic averaging to estimate the mean clutter power of background noise, the OS-CFAR processor, on the other hand, estimates the noise power from one of the N sorted

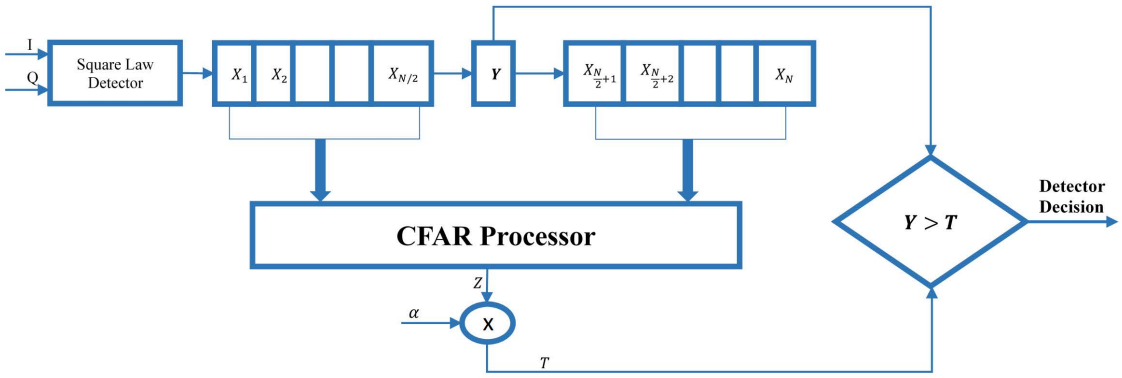

FIGURE 1. Typical architecture of CFAR processor.

observations in the reference window. The main reason for such a type of processing is to make the detector performance robust in the presence of interfering targets by avoiding complete reliance on arithmetic averaging of the observations. The test statistic Z selected to be the ordered reference window sample value is multiplied by the scale factor α, which controls the desired P_{fa} at a constant value. A decision is made by comparing the output of the sample under test (commonly called cell under test) Y with the adaptive threshold $T = \alpha Z$. The rank of order statistic can be any value in the range $1 \leq k \leq N$, and is typically chosen to maximize detection performance. For typical radar applications in Gaussian noise, the rank of order statistic providing a good background estimate is set such that $k = \frac{3N}{4}$ [31]. Because the OS-CFAR processor relies only on a single sample to estimate the noise power, its performance is often inferior to that of CA-CFAR processor in homogeneous environments. Therefore, another CFAR scheme has been introduced in the literature [20], [30]. This scheme takes advantages of both CA- and OS-CFAR schemes, which is the subject of our discussion in the next subsection.

D. THE TRIMMED MEAN (TM)-CFAR PROCESSOR

The TM-CFAR processor estimates the noise power by a linear combination of the ordered samples of reference window, which may be thought of as a generalization of the OS-CFAR scheme. It is anticipated that the linear combination may give better results because averaging will most likely estimate the noise power more efficiently as in the case of the CA-CFAR. In the TM-CFAR processor, the magnitudes of reference window samples are first ordered, and then T_1 cells (samples) from the lower end and T_2 cells (samples) from the upper end are trimmed. The trimming process is followed by summing the remaining ordered samples. In the TM-CFAR processor, the statistic Z is given by [30]

$$Z = \sum_{j=T_1+1}^{N-T_2} X_{(j)} \tag{1}$$

where $X_{(1)} \leq X_{(2)} \leq \ldots \leq X_{(N)}$ are the ordered reference window samples. An advantage of the TM-CFAR processor is that it reduces to the OS- and CA-CFAR processors by setting $(T_1, T_2) = (k-1, N-k)$ and $(0, 0)$, respectively. Furthermore, it reduces to the censored mean level detector (CMLD) by setting $T_1 = 0$ [30].

Note that the value of T_2 is not known a prior. In [24], automatic determination of an appropriate value of T_2 has been proposed using the maximum likelihood (ML) method. Let $k = N - T_2$. Therefore, the ML estimate of T_2 is determined from knowledge of the ML estimate of k, given below.

$$\widehat{k} = \underset{1 \leqslant k \leqslant N}{\arg\min} \{Q_{ML}(k)\} \tag{2}$$

where,

$$Q_{ML}(k) = k \ln(\gamma_1) + (N-k) \ln(\gamma_2) + N \tag{3}$$

$$\gamma_1 = \frac{1}{k} \sum_{i=1}^{k} X_{(i)} \tag{4}$$

$$\gamma_2 = \frac{1}{N-k} \sum_{i=k+1}^{N} X_{(i)} \tag{5}$$

The detection technique based on (2) is termed the automatic selection partial sum order statistic (ASPSOS)-CFAR.

E. SWITCHING (S)-CFAR PROCESSOR

The S-CFAR(S-CFAR) differs from the previous CFAR processors in that it exploits the cell under test to form two reference windows, from which the power of background noise is estimated [26]. Figure 2 shows the block diagram of the S-CFAR processor, where $X_1, X_2, \ldots, X_N$, are the reference window samples and Y is the cell under test. The parameter N_T is a threshold integer, while $\alpha > 0$, β_0, and β_1 are scaling factors to adjust the desired P_{fa}.

The first step in S-CFAR processor is to divide the samples of reference window into two sets: S_0 and S_1. The elements of S_0 are the samples of reference window whose amplitudes

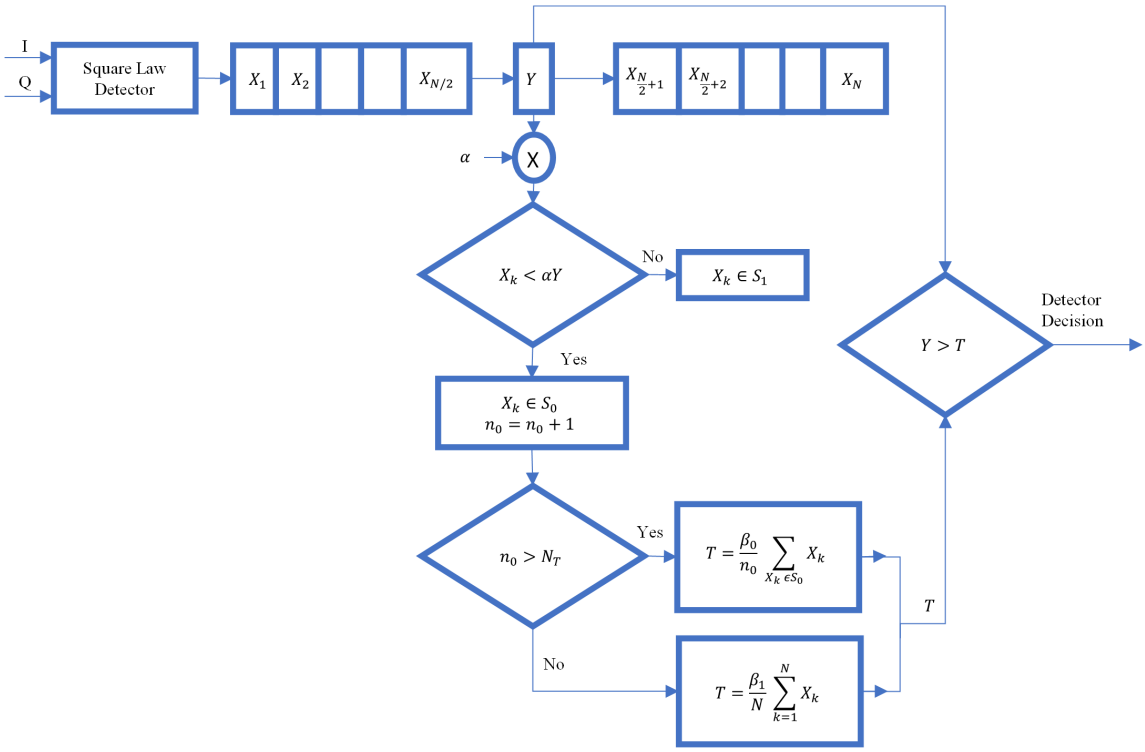

FIGURE 2. The S-CFAR processor.

are less than the threshold αY, while the remaining reference window samples constitute the elements of the set S_1. That is,

$$\text{If } X_k < \alpha Y, \quad S_0 \leftarrow X_k, \quad n_0 = n_0 + 1$$
$$\text{If } X_k > \alpha Y, \quad S_1 \leftarrow X_k$$

where $k = 1, 2, .., N$, and n_0 is initially equal zero. Based on the final value of n_0, the power of background noise is estimated either from the whole samples of S_0 or from the whole samples of reference window, denoted by S, and the result is multiplied by the scale factor β_0 or β_1, respectively, to produce the threshold T, which is then used to decide the presence or absence of a target. Specifically,

$$\text{If } n_0 > N_T, \quad T \leftarrow \frac{\beta_0}{n_0} \sum_{X_k \in S_0} X_k$$
$$\text{If } n_0 \leq N_T, \quad T \leftarrow \frac{\beta_1}{N} \sum_{k=1}^{N} X_k$$

The threshold T is then used to decide the presence or absence of a target. That is,

$$\text{If T} > \text{Y} \rightarrow \text{target is absent}$$
$$\text{If T} < \text{Y} \rightarrow \text{target is present}$$

It is worthy noting that the set S_0 is selected to estimate the noise power if the number of its elements, denoted by n_0, is greater than N_T. This is to guarantee that S_0 has enough number of samples to perform reliable estimation. When $n_0 \leq N_T$, this means that the cell under test has small amplitude, and therefore the whole samples of reference window is used to provide better estimate of noise power. Note that the design parameters of S-CFAR processor can be tuned such that its performance in an i.i.d Gaussian noise environment has almost no degradation compared to that of the CA-CFAR. Yet, it has the detection advantages of other existing CFAR processors in the presence of strong interfering targets.

Two variants of the S-CFAR processor are of particular interest here, as they combine the concept of switching and ordering operations together. The first approach, [33], is the switching ordered statistic CFAR type I (SOS-CFAR I). As in the S-CFAR processor, it switches between the set S_0 and the set S containing the whole samples of reference window, and this switching operation is done depending on the value of n_0. The main difference between the S-CFAR and SOS-CFAR I processors is in that the samples of S_0 and S in SOS-CFAR I are first ordered, and the k^{th} smallest element of either S_0 or S is then selected to estimate the noise power.

The generalized switching (GS)-CFAR processor is another variant of S-CFAR processor [34]. It works in a similar manner, as in the S-CFAR processor, but differs in that it orders the samples of reference window first, and then estimates the noise power from the set S using the k^{th} smallest element of its ordered samples for the case $n_0 \leq N_T$.

Table 1 shows the computational complexities of different CFAR processors evaluated at the worst computational case when all samples of reference window are below the sample under test, Y. For simplicity of presentation, the ln(.)

TABLE 1. Computational complexities of different CFAR processors.

CFAR Algorithms	Math Operations			
	No. of Additions	No. of Multiplications and Divisions	No. of Comparisons	No. of Sorted Samples
CA-CFAR	N	1	1	-
OS-CFAR	-	1	1	N
ASPSOS-CFAR	$N(N+1)$	$6N+1$	N	N
TM-CFAR	$N-T_1-T_2$	1	1	N
S-CFAR	$2N$	3	$N+2$	-
SOS-CFAR I	N	2	$N+2$	N
GS-CFAR	$2N$	3	$N+2$	N

operation of the ASPSOS-CFAR is assumed pre-computed and stored in a look-up table for values in the range of interest, and therefore it is not taken into consideration in our analysis. Here, the number of arithmetic operations to produce one decision is used to measure the computational complexity of different CFAR processors. This includes the number of additions, multiplications/divisions, comparisons, and sorted samples. From the table, it is clear that all CFAR algorithms, except ASPSOS-CFAR, have relatively comparable numbers of addition, multiplication, division, and comparison operations. However, the ASPSOS-CFAR has the highest computational complexity, while the CA-CFAR is the most efficient. On the other hand, it is observed that the S-CFAR has an advantage over the OS-, ASPSOS-, TM-, SOS-, and GS-CFARs in that it does not have sorting operation.

III. PN ACQUISITION USING SMART ANTENNA

The determination of detector threshold for PN code acquisition is a major concern in DS-CDMA systems so that optimum performance is maintained [35], [36]. This section proposes the utilization of smart antenna and S-CFAR processor for the development of a simple and practical PN code acquisition system. Note that the utilization of smart antennas in CDMA communications has several benefits. In particular, smart antenna adapts beam shape to enhance the desired signal, expand range coverage, and suppress signals of other users arriving from different directions. Furthermore, it tracks multiple users by steering multiple beams [37]. On the other hand, the CFAR processor is used to adapt to the variation in noise power and suppress the effect of multipath interference to reduce false alarms for efficient PN code acquisition [23].

This section is organized as follows. Subsection A presents a brief introduction to smart antenna. Subsection B presents the system model for PN acquisition in CDMA communication. Subsection C presents the S-CFAR processor in the context of PN acquisition. Performance of the proposed scheme is theoretically analyzed in Subsection D, where closed form expressions are derived for P_{fa} and P_d. Knowing P_{fa} and P_d facilitates straightforward evaluation of system performance in terms of average acquisition time (T_{acq}).

A. SMART ANTENNA SYSTEM

Smart antenna systems can be classified into two main categories. The first category is called fixed multiple beams. Sometimes, it is also called switched beam arrays. The other category is the adaptive antenna arrays. In both cases, the main function of a smart antenna is to maximize the gain of main beam and steer it in the direction of an intended user, and at the same time suppress interfering signals from other directions [19].

The main idea of operation of a switched beam antenna array is to switch among the beams and select the beam corresponding to the desired direction for transmission or reception. Switched beam antennas are subject to degradation by the presence of unwanted signals or multipath interference. Adaptive antenna arrays (or adaptive beamformers), on the other hand, use signal processing algorithms to shape the beam pattern according to certain conditions for the purpose of maximizing the arrays gain in the direction of a particular user and minimizing it in the direction of other interfering signals. Therefore, some sort of intelligence is incorporated into their control system. A basic implementation often considered for adaptive beamforming is the linear equally spaced array configuration [38].

B. SYSTEM MODEL

The system model considered in this work follows the system model presented in [18], as depicted in Figure 3 with the following difference. The model of [18] uses fixed thresholding, while our model uses CFAR detector. Therefore, the two models are identical, except in the last block pertaining to thresholding.

Figure 3a shows the in-phase (I) and quadrature-phase (Q) components of PN correlator, while Figure 3b shows the whole system model in a compact complex representation form, which consists of a smart antenna, adaptive algorithm to adjust the weights of beamformer, and a CFAR processor. This setup exploits all array elements' outputs for PN acquisition. The linear array elements are equally spaced with a distance (d) between any two elements. The distance d is constrained to be at most half a wavelength ($\lambda/2$) [38]. For $d = \lambda/2$, the signal $y_m''(t)$ of a desired user, received from the m^{th} antenna element of the array, is given by [18],

$$y_m''(t) = \sqrt{2P}\eta(t)\, b(t-\tau T_c)\, c(t-\tau T_c) \times e^{j(\omega_c t+\phi_m)} e^{j\xi(t)} e^{-j\pi(m-1)\sin\varphi} + n_{bm}(t) \quad (6)$$

where P denotes the power of received signal, $b(t)$ is the information data, T_c is a chip interval, $c(t)$ is the PN code signal, $\eta(t)$ and $\xi(t)$ are the fading amplitude and phase, respectively, ω_c is the angular carrier frequency, ϕ_m is the carrier phase, and τ is an incoming PN code phase offset from the receiver PN code phase. The φ is an incidence angle, which is measured from the normal to the linear array. The term $n_{bm}(t)$ accounts for a bandpass AWGN and any other interfering signal at the m^{th} element. In what follows, $b(t)$ is set equal to 1 for all values of t, assuming a pilot channel is employed.

The received signal $y_m''(t)$ is first down converted to baseband by multiplication by the reference waveform $e^{j\omega_c t}$.

The resultant signal $y'_m(t)$ is then passed through the filter $H^*(f)$, which is designed to match the chip pulse. Therefore, the equivalent baseband discrete-time signal $y_m(i)$ is formed by sampling the output of matched filter at the chip rate $1/T_c$. That is,

$$y_m(i) = \sqrt{E_c}\eta(i)\, c(i-\tau)\, e^{j[\phi_m+\xi(i)-\pi(m-1)\sin\varphi]} + n_m(i), \quad m = 1, 2, \ldots, M \tag{7}$$

where E_c is the chip energy, and $n_m(i)$ is the sample of a complex valued zero-mean AWGN at the i^{th} chip time. A frequency non-selective, slow Rayleigh fading channel is assumed between the intended user's transmitter and the antenna array; hence, the fading amplitude and phase shift are kept constant ($\eta(i) = \eta$ and $\xi(i) = \xi$) over the observation interval of length LT_c, where L is an integer.

The output of PN correlator is the input to the beamformer, whose value at time iT_c for the m^{th} antenna element, is given by

$$r_m(i) = \sum_{i'=0}^{i} y_m(i')\, c(i'-\tau'), \quad m = 1, 2, \ldots M \tag{8}$$

where τ' is the phase of local PN code, and $i = 0, 1, 2, \ldots, L-1$. Let the signal $g(i)$ be defined as follows.

$$g(i) = \sum_{m=1}^{M} w_m{}^*(i)\, \frac{r_m(i)}{\sqrt{\frac{1}{M}\sum_{j=1}^{M} r_j^*(i)\, r_j(i)}} \tag{9}$$

where $w_m(i)$ is the associated weight of the m^{th} branch at time iT_c. The adaptive beaformer will work on the samples of signal $g(i)$ for minimizing its output average power while maintaining a fixed gain along the direction of a desired signal. Therefore, under the assumption of perfect synchronization and noiseless channel, $g(i) = M$ if $w_m(i)$ is set such that

$$w_m(i) = e^{-j[\phi_m+\xi(i)-\pi(m-1)\sin\varphi]} \tag{10}$$

Note that the optimum beamformer weights can be computed iteratively using the least-mean-square (LMS) algorithm, to achieve minimum square error (MSE) between a desired value and the beamformer output. The LMS algorithm is simple to implement, as weights update equation is given by [18]

$$w_m(i+1) = w_m(i) + \mu e^*(i)\, \frac{r_m(i)}{\sqrt{\frac{1}{M}\sum_{j=1}^{M} r_j^*(i)\, r_j(i)}} \tag{11}$$

where μ denotes the convergence parameter of the algorithm, and $e(i)$ is the error between the beamformer output and the target value M. Hence,

$$e(i) = M - g(i) \tag{12}$$

At time $i = L-1$, the LMS is expected to coverage, and the antenna array spatial correlation output z_0 is computed using the weights $w_m(L-1)$ and the last accumulation output $r_m(L-1)$ as follows.

$$z_0 = \frac{1}{ML}\sum_{m=1}^{M} w_m^*(L-1)\, r_m(L-1) \tag{13}$$

In the next section, the final decision variable Z defined below is used to set the adaptive threshold of proposed S-CFAR processor. The statistic Z is defined as

$$Z = |z_0|^2 \tag{14}$$

C. ADAPTIVE CFAR THRESHOLDING

Thresholding is applied to the statistic Z of Figure 3 to take decision with respect to PN synchronization. Therefore, it affects the performance of the proposed PN acquisition system. The S-CFAR processor is considered here to implement the adaptive operation of the decision operation. In particular, the threshold parameters of S-CFAR processor are selected to adapt according to the magnitude of the correlation between the locally generated PN sequence and the incoming signals. The block of adaptive thresholding of Figure 3 is detailed in Figure 4, where the beamformer's output samples are serially fed into a shift register of length $N+1$. The current output of beamformer, denoted by Z, is stored in the first shift register. The set of previous beamformer outputs, denoted by $Z_j (j = 1, 2, \ldots, N)$, represent the S-CFAR reference window samples. A PN code acquisition is declared if Z is greater than a threshold T. The threshold T is determined by processing the samples of reference window to maintain a constant P_{fa}, as described in Section II.E. On the other hand, if Z is less than the threshold T, the test is automatically repeated at the next offset position of local code phase [20].

D. PERFORMANCE METRICS

In this subsection, we consider the commonly used metrics to evaluate the performance of proposed S-CFAR-based PN acquisition system, following the approach of [18]. These metrics include the P_d, P_{fa}, and T_{acq}. For P_d and P_{fa}, closed form expressions are derived, which can straightforwardly be used to compute the third metric pertaining to the average acquisition time.

The mathematical expression for P_{fa} can be determined if the probability density function (PDF) of statistic Z is known for the case when the incoming and locally generated PN codes are not synchronized. That is,

$$c(i-\tau) \neq c(i-\tau') \tag{15}$$

The beamformer weights $w_m(i)$, under such a condition, may converge to random values, and the PDF of Z takes the form [18]

$$f_Z(z/H_0) = \frac{1}{MLI_0} e^{\frac{-z}{MLI_0}} \tag{16}$$

where $I_0/2$ is the additive noise power. On the other hand, the P_d is derived for the case where

$$c(i-\tau) = c(i-\tau') \tag{17}$$

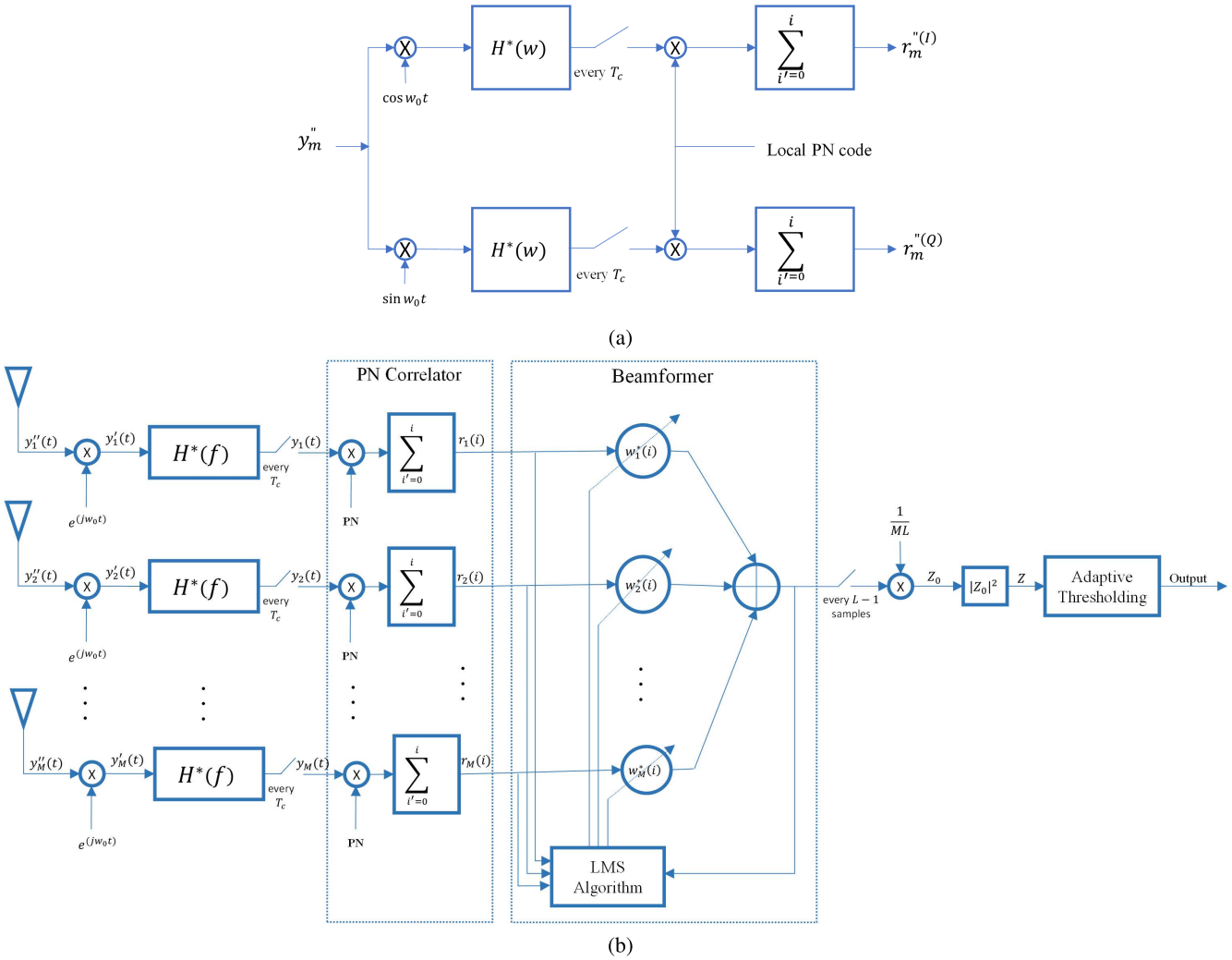

FIGURE 3. (a) Inphase (I) and quadrature (Q) components of PN correlator. (b) Block diagram of the proposed PN code acquisition scheme.

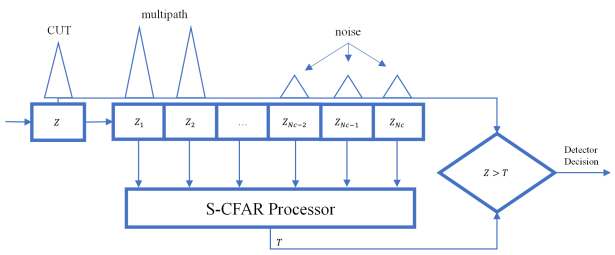

FIGURE 4. S-CFAR processor.

Under codes synchronization, the smart antenna achieves perfect track of the direction of arrival of the desired user; hence, we have

$$w_m = e^{-j[\phi_m + \xi(i) - \pi(m-1)\sin\varphi]} \tag{18}$$

The PDF of statistic Z for such a case was derived in [18], and is given by

$$f_Z(z/H_1) = \frac{1}{MLI_0 + M^2L^2E_c\eta^2} e^{\frac{-z}{MLI_0 + M^2L^2E_c\eta^2}} \tag{19}$$

where η^2 denotes the fading channel power. Note that both PDFs follow an exponential distribution with parameter γ; that is,

$$\gamma = \begin{cases} MLI_0, & \text{under } H_0 \\ MLI_0 + M^2L^2E_c\eta^2, & \text{under } H_1 \end{cases} \tag{20}$$

Let $\gamma_n = MLI_0$. Therefore, we can write γ under H_1, as follows.

$$\gamma = \gamma_n \left(1 + ML\ SNR_c\ \eta^2\right) \tag{21}$$

where $SNR_c = E_c/I_0$ is the signal-to-noise ratio per chip. If the received samples contain multipath interference with an average interference-to-noise ratio of $INR = I_i/I_0$, then

$$\gamma = \gamma_n \left(1 + ML\ INR\ \eta^2\right) \tag{22}$$

In [26], description and closed-form analysis of the S-CFAR algorithm for radar target detection in a non-homogeneous environment has been developed. The analysis assumed targets detection in a Rayleigh background, which

means that the square-law detected samples are exponentially distributed. Therefore, with a proper modification of the results reported in [26], the probability of detection of proposed PN acquisition system, employing S-CFAR processor, can be derived and is given by, (23), as shown at the bottom of the page, where $M_0 = \max(0, n_0 - N + M)$, $N_T = N - \text{noI} - 1$, and noI is the number of reference samples corrupted by multipath interreference. The functions $V(k, n)$ and $H(k, n)$ are defined as (24) and (25), shown at the bottom of the page, in which $\zeta_{k,n}$, $\rho_{k,n}$ and $\xi_{k,n}$ are given by

$$\zeta_{k,n} = N\beta_I^{-1} - (N - n_0 + k + n), \qquad \alpha \geqslant 0 \tag{26}$$

$$\rho_{k,n} = \alpha \left[\frac{M - m + k}{1 + ML\ INR\eta^2} + N - M - n_0 + m + n \right] \tag{27}$$

$$\xi_{k,n} = n_0\beta_0^{-1} - (k + n), \qquad \alpha \geqslant 0 \tag{28}$$

It is of interest to note that P_d of S-CFAR given by (23) is a function of three scaling parameters (α, β_0, and β_1), while the detection probabilities of other CFARs presented in Section II (i.e. CA-, OS-, CMLD) are functions of only one scaling parameter. Therefore, the S-CFAR has more degrees of freedom to optimize its performance. In particular, the three parameters of S-CFAR can be tuned for the same P_{fa} to give P_d better than those of other CFARs, as demonstrated in Section IV.

The probability of false alarm can be obtained from (23) by setting $SNRc = INR = 0$. Hence, the acquisition time T_{acq}, is given by [18]

$$T_{acq} = \frac{(2 - P_d)\left(1 + K_p P_f\right)(R - 1)}{2P_d} + \frac{1}{P_d} \tag{29}$$

where K_p denotes a fixed penalty factor and R is the size of the search range of the PN code phase. The unit of T_{acq} is LT_c.

IV. RESULTS AND DISCUSSION

This section aims to analyze the proposed PN acquisition scheme for DS-CDMA wireless communications in a multipath Rayleigh slowly fading channel. Numerical and simulation results have been presented to:

- ensure that the P_{fa} of S-CFAR processor will keep its value constant, independent of the level of noise, correlation length, and number of antennas. This is to confirm that the switched algorithm is truly CFAR processor. Effects of S-CFAR's threshold parameters on P_{fa} have been also considered.
- study the effects of different design parameters on P_d and T_{acq}, which include the number of antennas, S-CFAR's threshold parameters, length of reference window, correlation length, and number of interfering cells resulting from multiple access interference.
- compare the performance of proposed S-CFAR processor with other CFAR algorithms previously proposed for PN acquisition for DS-CDMA systems.

In our numerical and simulation results, a uniform linear array is considered with spacing of half wavelength between the antenna elements. The number of antenna elements (M) is chosen to be 1, 3, and 5. The effect of reference window size (N), observation interval or correlation length (L), the thresholds (α, T), and SNR/chip on P_{fa},P_d, and T_{acq} are considered. The results are given for spreading factor $L_s = 127$, chip rate equal 1.2288 Mcps, unity average fading channel power, and $E_c/I_0 = 10E_c$, where E_c is the information chip energy and $I_0 = 0.1$ is the noise power. The thresholds α and T are chosen to guarantee that $P_{fa} = 0.001$.

A. PROBABILITY OF FALSE ALARM

The false alarm probability is plotted against the noise power (in dB) for $N = 16$, $L = 127$, noI $= 0$, and $M = 1, 3$, and

$$\begin{aligned} &P_d\left(N, N_T, \alpha, \beta_0, \beta_1, M, L, SNR_c, INR, \eta\right) \\ &= \frac{1}{1 + MLSNR_c\eta^2} \sum_{n_0=0}^{N_T} \sum_{m=M_0}^{\min(M,n_0)} \sum_{n=0}^{n_0-m} \sum_{k=0}^{m} \left\{ \binom{M}{m} \binom{N-M}{n_0-m} \binom{n_0-m}{n} \binom{m}{k} \times \frac{(-1)^{k+n} V(k,n)}{\left(1 + MLINR\eta^2\right)^M} \right\} \\ &\quad + \frac{1}{1 + MLSNR_c\eta^2} \sum_{n_0=N_T+1}^{N} \sum_{m=M_0}^{\min(M,n_0)} \sum_{n=0}^{n_0-m} \sum_{k=0}^{m} \left\{ \binom{M}{m} \binom{N-M}{n_0-m} \binom{n_0-m}{n} \binom{m}{k} \times \frac{(-1)^{k+n} H(k,n)}{\left(1 + MLINR\eta^2\right)^m} \right\} \end{aligned} \tag{23}$$

$$V(k,n) = \frac{\zeta_{k,n}^N \left[1 - \frac{\zeta_{k,n} ML\ INR\eta^2}{1 + ML\ INR\eta^2} \right]^{-M}}{\left[\rho_{k,n} + \left(1 + ML\ SNR_c\eta^2\right)^{-1} \right] \times \left[\zeta_{k,n} + \rho_{k,n} + \left(1 + ML\ SNR_c\eta^2\right)^{-1} \right]^{N-M}} \tag{24}$$

$$H(k,n) = \frac{\xi_{k,n}^{n_0} \left[1 - \frac{\xi_{k,n} ML\ INR\eta^2}{1 + ML\ INR\eta^2} \right]^{-m}}{\left[\rho_{k,n} + \left(1 + ML\ SNR_c\eta^2\right)^{-1} \right] \times \left[\xi_{k,n} + \rho_{k,n} + \left(1 + ML\ SNR_c\eta^2\right)^{-1} \right]^{n_0-m}} \tag{25}$$

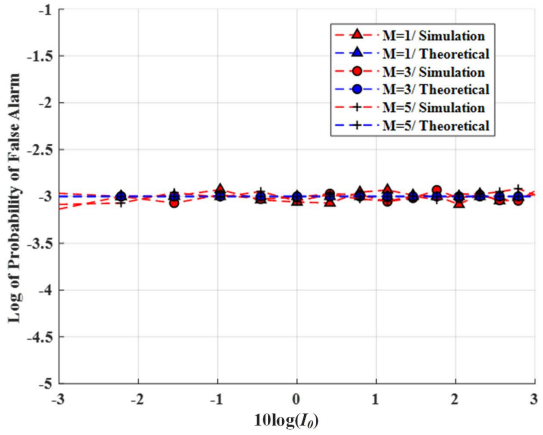

FIGURE 5. Log(P_{fa}) versus 10log(I_0) for different number of antennas.

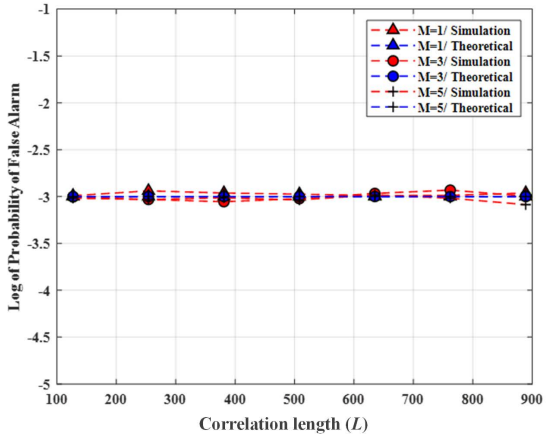

FIGURE 6. Log(P_{fa}) versus correlation length for different number of antennas.

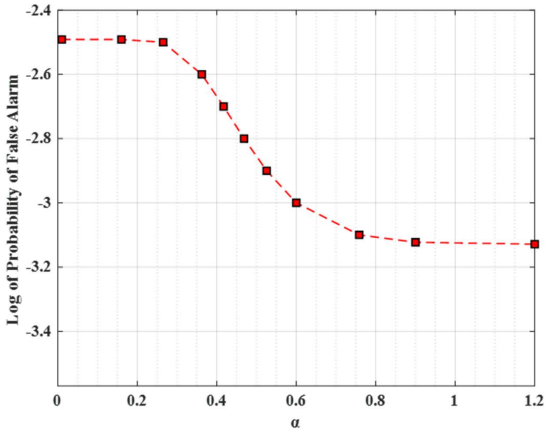

FIGURE 7. Log(P_{fa}) at different level versus (α).

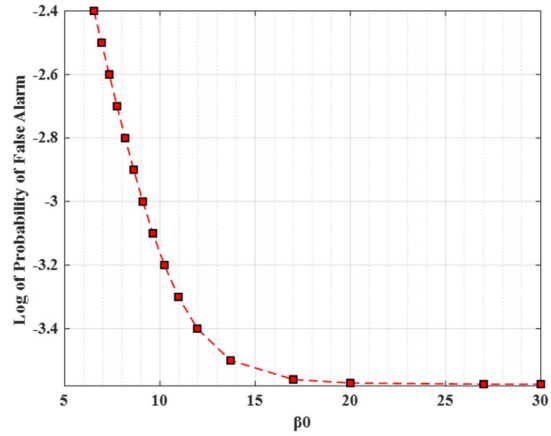

FIGURE 8. Log(P_{fa}) at different levels versus (β_0).

5 using the S-CFAR adaptive threshold scheme. The results are displayed in Figure 5. For the numerical and simulation results, the processor's parameters were fixed at $(\alpha, \beta_0, \beta_1) = (0.6, 9.1, 6.9)$, which result in a constant probability of false alarm rate, over a range of I_0 values. For convenience, log of P_{fa} is considered. It is obvious from Figure 5 that the theoretical and simulated P_{fa} are closely matched.

Next, we consider the effect of: i) correlation length L, and ii) S-CFAR parameters $(\alpha, \beta_0, \beta_1)$ on the probability of false alarm. Figure 6 shows P_{fa} against the correlation length with $L = 127, 254, 381, 508, 635, 762$, and 889, $N = 16$, noI $= 0$, and $M = 1$, 3, and 5. The noise power was fixed at 0.1. By virtue of Figure 6, it is clear that P_{fa} is independent of observation interval or correlation length for different values of M. Therefore, the proposed PN acquisition scheme is capable of maintaining constant false alarm rate at different signal processing scenarios.

The P_{fa} is also plotted against the parameters $(\alpha, \beta_0, \beta_1)$ for $M = 3$, $I_0 = 0.1$, noI $= 0$, $N = 16$, and $L = 127$. Figures 7 to 9 show the results when two parameters are fixed while the third is varied. It is observed from the figures that P_{fa} has zero rate of change for values of α less than 0.22 and greater than 0.87 and varies with a rate of 0.2 in-between. The P_{fa} varies approximately with 0.2 rate of change for values of β_0 less than 12, then this rate starts decreasing after value of $\beta_0 = 12$ and becomes almost constant for $\beta_0 \geqslant 24$. Similarly, the P_{fa} has 0.2 rate of change for values of $\beta_1 \leq 6.9$. For values of β_1 greater than 6.9, the rate of change of P_{fa} slows down and becomes constant after $\beta_1 \geqslant 10$. In conclusion, increasing the value of a parameter above certain threshold, while the other two parameters are fixed, saturates the P_{fa} and pushes it to be at a constant level.

Figure 10 shows the variation of P_{fa} in terms of the two parameters α and β_0, where β_1 is fixed at (8.6388) to facilitate visualization of the results. This figure indicates that there are several parameter's values which give $P_{fa} = 0.001$. Next, we show that different values of parameters satisfying a fixed P_{fa} may not lead to the same P_d. Therefore, the user of S-CFAR should choose those parameters maximizing the P_d.

B. PROBABILITY OF DETECTION

Here, we assist the performance of proposed acquisition scheme in terms of P_d. In particular, P_d is plotted against SNR/chip (in dB) for $N = 16$, $L = 127$, noI $= 0$, and

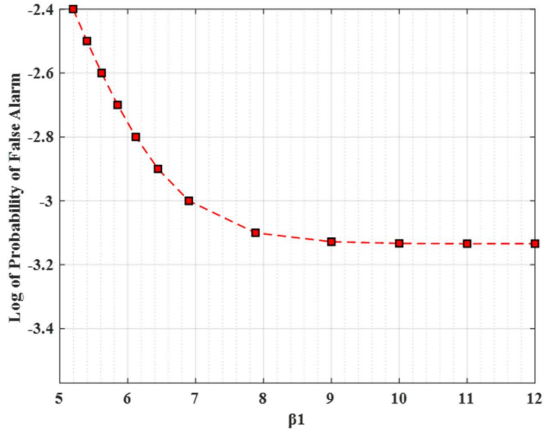

FIGURE 9. Log(P_{fa}) at different levels versus (β_1).

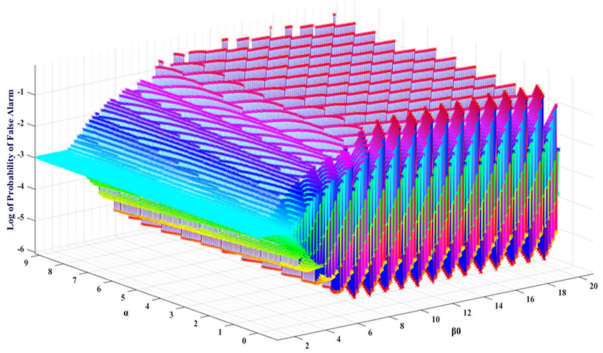

FIGURE 10. Log(P_{fa}) versus values of parameters (α, β_0), where $\beta_1 = 8.6388$.

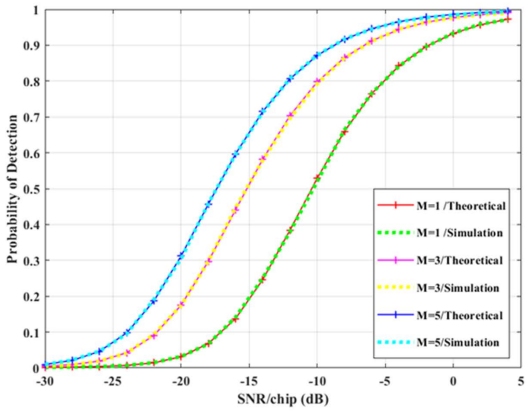

FIGURE 11. P_d versus SNR/chip in (dB) for different number of antennas.

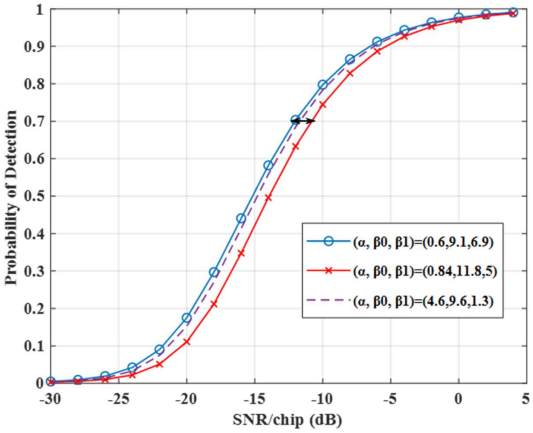

FIGURE 12. P_d versus SNR/chip in (dB) using different parameters' values.

$M = 1, 3$, and 5. The parameters of S-CFAR scheme have been set equal to those used to produce Figure 5. The P_d is computed theoretically from Eq. (23) and by simulations, and the results are displayed in Figure 11. It is observed from the figure that the two results are closely matched. Another observation is that P_d gets improved as the number of antennas increases. However, the improvement in P_d becomes more clearer when comparing with the case where $M = 1$. Note that the saving in SNR/chip at $P_d = 0.6$ may reach 4 dB using $M = 3$, and 7 dB using $M = 5$.

Next, we consider the effect of S-CFAR parameters (α, β_0, β_1) on the probability of detection. Figure 12 shows P_d as a function of SNR/chip for noI z 0, $M = 3$, $N = 16$, and $L = 127$. The P_d is plotted for various parameters values, where we observe that three sets of which produce comparable performances. For example, the sets (α, β_0, β_1) = (0.6, 9.1, 6.9), (4.6, 9.6, 1.3), and (0.84, 11.8, 5) produce $P_d = 0.7$ at SNR/chip = -12.05, -11.7, and -10.8 dB, respectively. The difference in performance between the first and third sets of parameters is 1.25 dB, which is relatively tangible. This asserts the importance of properly selecting the parameters values of the S-CFAR scheme.

The probability of detection for different reference window sizes are shown in Figure 13. Assuming no interfering cells, the number of antennas $M = 3$, and correlation length $L = 127$, the figure shows that increasing the reference window size N improves the probability of detection and decreases the CFAR loss. However, as the value of N increases the effect on the P_d becomes less pronounced. By virtue of Figure 13, we observe that at $P_d = 0.52$ the CFAR loss is 0.9 dB when N is reduced from 16 to 8, while the CFAR loss is only 0.1 dB for the case when N is reduced from 32 to 24.

Multipath interreference is an effective parameter which manifests itself in the form of corrupting cells in the reference window of PN acquisition systems for DS/CDMA wireless communications. Figure 14 indicates that the proposed system of PN acquisition using smart antenna and S-CFAR processor suffers performance degradation and reduction in probability of detection as the number of interfering cells increases. The results of Figure 14 are produced using $N = 16$, $M = 3$, $L = 127$, and INR = SNR/chip. However, the performance can be enhanced by using larger number of antennas, as demonstrated in Figure 15 for the two cases $M = 3$ and 5 when noI = 5.

The last parameter to be investigated in this subsection is the effect of correlation length L on the probability of

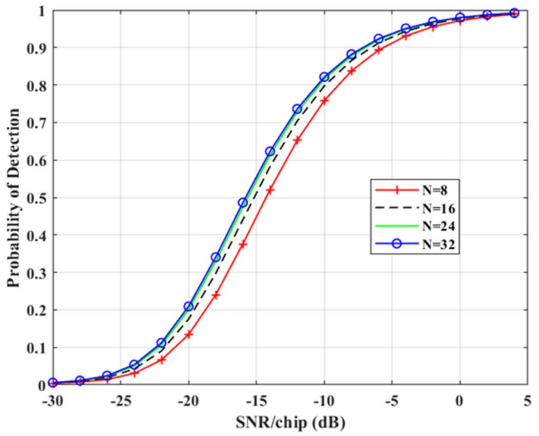

FIGURE 13. P_d versus SNR/chip in (dB) for different reference window sizes.

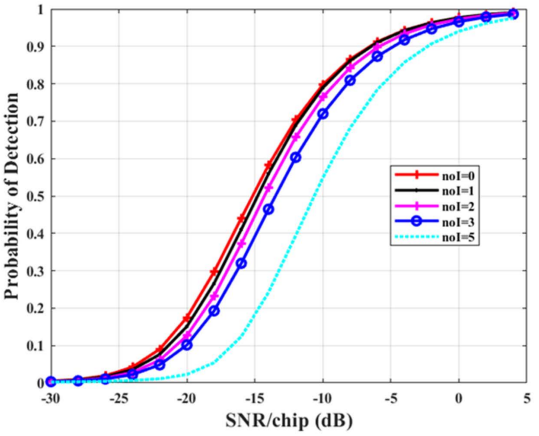

FIGURE 14. P_d versus SNR/chip in (dB) for different number of interfering cells.

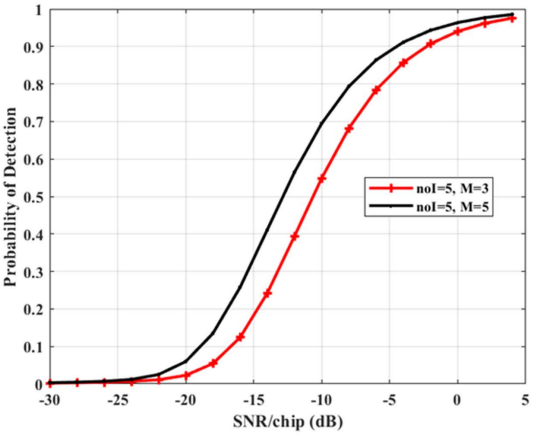

FIGURE 15. P_d versus SNR/chip in (dB) for noI = 5, M = 3 and 5.

detection P_d. Figure 16 shows P_d for different values of L when $N = 16$, $M = 3$, and noI $= 0$. Note that the probability of detection is improving as the correlation length increases. It is of interest to note that the probability of detection for $M = 3$ and $L = 127$ is the same as that of $M = 1$ and

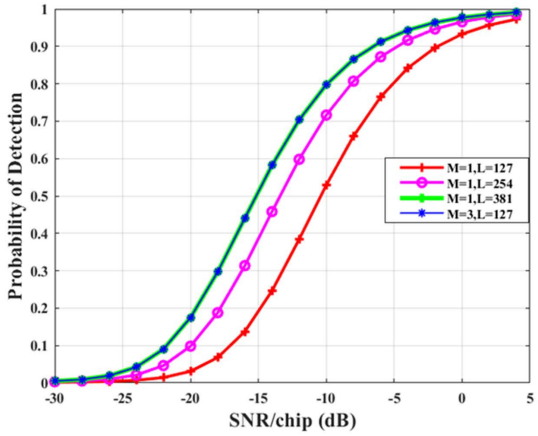

FIGURE 16. P_d versus SNR/chip in (dB) for noI = 5, M = 3 and 5.

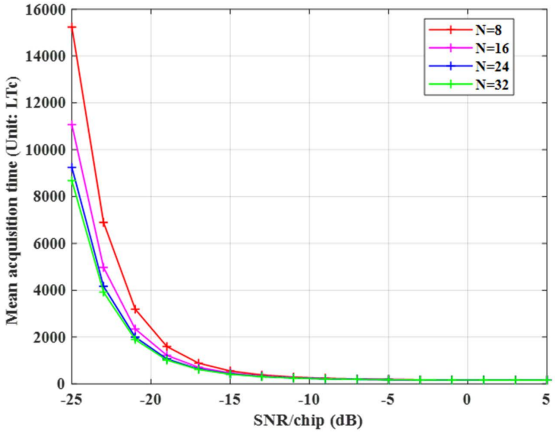

FIGURE 17. T_{acq} versus SNR/chip (dB) for different sizes of reference window.

$L = 381$. This is intuitively not surprising because L affects the PDF of decision variable Z, given in Eq. (19), in a similar manner to what M does.

C. MEAN ACQUISITION TIME

The elapsed acquisition time in serial search for PN acquisition using smart antenna and adaptive thresholding of S-CFAR algorithm is defined in Eq. (29). In this subsection, the performance of proposed acquisition system is investigated against SNR/chip for different number of antennas and different reference window's sizes. The numerical results are computed for observation interval, PN code phase search range, and penalty factor equal to 255, in a similar manner as in [18]. The unit of T_{acq} is LT_c, where T_c is the chip duration.

The effect of window size on T_{acq} is displayed in Figure 17 for number of antennas $M = 3$. As previously demonstrated in Figure 13, larger window size improves the probability of detection. This is consistent with the results of Figure 17, where we observe that the mean acquisition time T_{acq} is improving (i.e. decreasing) as the window size N increases, especially at low SNR/chip values. However, the behavior

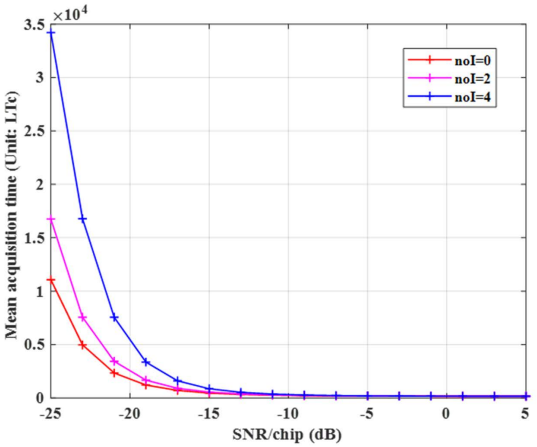

FIGURE 18. T_{acq} versus SNR/chip (dB) for different sizes of reference window.

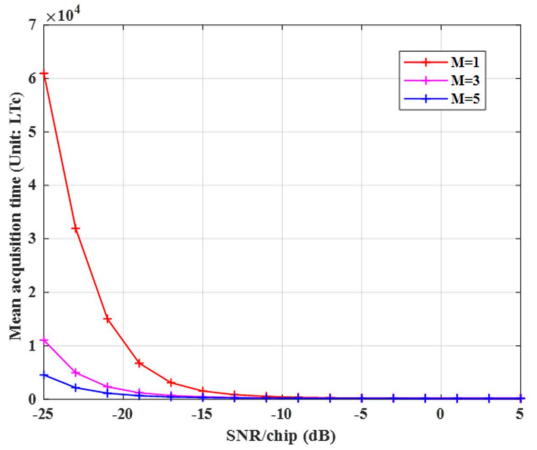

FIGURE 19. T_{acq} versus SNR/chip (dB) for different number of antennas.

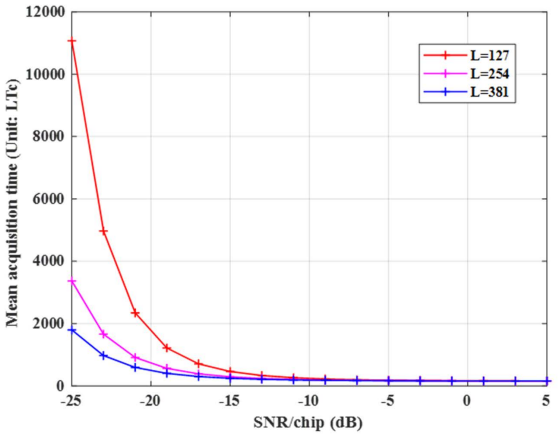

FIGURE 20. T_{acq} versus SNR/chip (dB) for different values of correlation length.

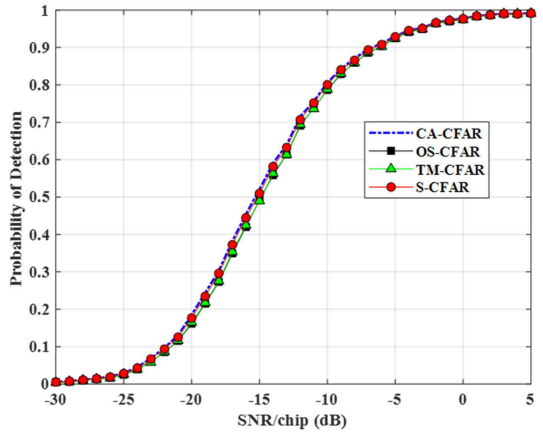

FIGURE 21. P_d versus SNR/chip in (dB) for different CFAR algorithms, noI = 0.

of T_{acq} is almost the same, for the four values of N, for SNR/chip>-10dB.

Figure 18, on the other hand, shows T_{acq} for $N = 16$, $M = 3, L = 127$ and number of interfering cells noI = 0, 2, and 4. Based on the figure, increasing the number of interfering cells affects the system performance and causes an increase in the acquisition time T_{acq}. This observation goes along the results demonstrated in Figure 14, where an increase in the number of interfering cells decreases the probability of detection of the proposed system.

Figure 19 shows the effect of number of antennas on T_{acq} with $N = 16$ and no interfering cells. It is obvious from the figure that increasing the number of antennas improves the mean acquisition time. At $T_{acq} = 4564.67\ LT_c$, we observe 5dB and 7dB improvement in SNR/chip for $M = 3$ and $M = 5$, respectively, compared to the case $M = 1$. It is relevant here to mention that the correlation length has same effect on the mean acquisition time as the number of antennas does. The results of Figure 20 demonstrate this assertion, where the mean acquisition time decreases or improves as the correlation length increases. The results are plotted for $N = 16$, $M = 3$, and $L = 127$, 254, 381, and no interfering cells.

D. COMPARISONS WITH OTHER CFAR PROCESSORS

Different CFAR algorithms have been studied for PN acquisition using smart antennas for DS/CDMA mobile communications. The first class of processors relies solely on the reference window samples to define the adaptive threshold. This class includes the CA-CFAR, OS-CFAR, ASPSOS-CFAR, and TM-CFAR processors previously introduced in Section II. The second class of processors exploits both the reference window samples and the cell under test to determine appropriate thresholds to maintain constant false alarm rate. This class includes S-CFAR, SOS-CFAR I, and GS-CFAR processors. In this subsection, we compare the performance of S-CFAR with both processors' classes at fixed $P_{fa} = 0.001$. Therefore, the threshold(s) of each processor is adjusted accordingly to produce such a constant false alarm rate.

Figures 21 to 23 show the probability of detection of PN acquisition system employing smart antennas and CA-CFAR,

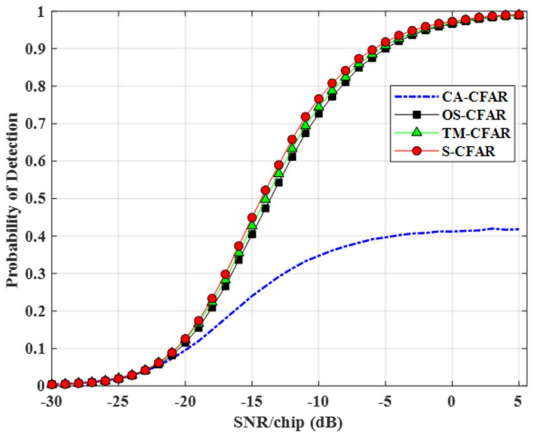

FIGURE 22. P_d versus SNR/chip in (dB) for different CFAR algorithms, noI = 2.

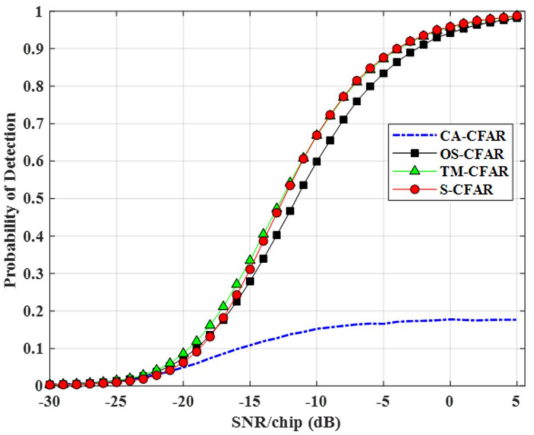

FIGURE 23. P_d versus SNR/chip in (dB) for different CFAR algorithms, noI = 4.

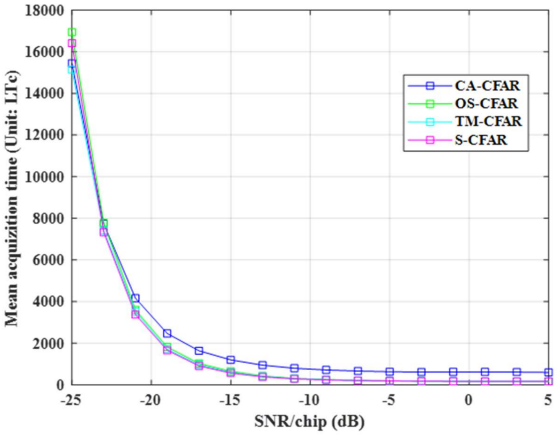

FIGURE 24. T_{acq} versus SNR/chip (dB) for different CFAR algorithms, noI = 2.

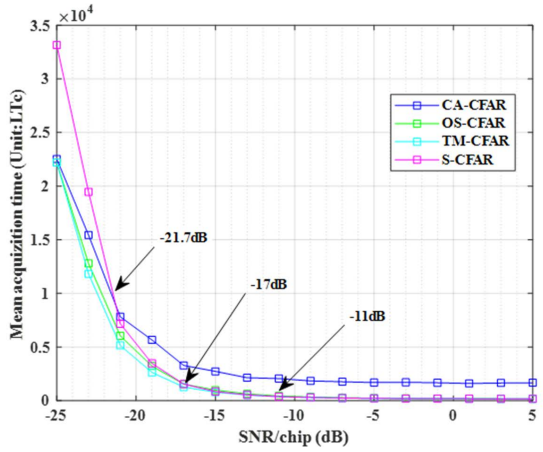

FIGURE 25. T_{acq} versus SNR/chip (dB) for different CFAR algorithms, noI = 4.

OS-CFAR ($k = 3N/4$), TM-CFAR ($T_1 = 0, T_2 = 4$), and S-CFAR algorithms. The reference window size is set to $N = 16$, number of antennas $M = 3$, and correlation length $L = 127$, and number of interfering cells (noI = 0, 2, 4). Note that the CA-CFAR performance is optimum in homogeneous environment, but with the existence of an interference, the performance suffers a sever degradation, as shown in Figure 22. The other CFAR algorithms' performances are very much similar in the case of noI = 0, although S-CFAR has slight better performance than TM-CFAR and OS-CFAR.

When the number of interfering cells is set to noI = 2, 4, the performance of different processors is quite pronounced, as shown in Figures 22 and 23. That is, TM-CFAR has better performance than OS-CFAR in both cases of noI = 2, 4. For the S-CFAR, it has better performance than the other two processors when noI = 2. In the case of noI = 4, as shown in Figure 23, the TM-CFAR has better performance than S-CFAR at small values of SNR/chip up to -11 dB, and the two processors maintain almost the same performance for greater values of SNR/chip.

Figure 24 shows the corresponding mean acquisition time of each processor with $N = 16, L = 127, M = 3$ and noI = 2 and 4. It is observed 0.65, 0.75, 0.8dB improvements in SNR/chip for OS-CFAR, TM-CFAR, and S-CFAR processors, respectively, compared to the case of CA-CFAR processor at $T_{acq} = 3500LT_c$ and noI = 2. But in the existence of 4 interfering cells, as shown in Figure 25, the S-CFAR suffers a degraded performance in low values of SNR compared to TM-CFAR, OS-CFAR, and CA-CFAR, which can be summarized as follows. The S-CFAR processor shows better performance than CA-CFAR for SNR/chip values above -21.7dB. Similarly, it starts to achieve better acquisition time than OS-CFAR for SNR/chip values above -17dB. While it has almost same T_{acq} as that of TM-CFAR when SNR/chip values are above -11.4 dB.

Figure 26 shows the probability of detection of PN acquisition system employing smart antennas, S-CFAR, and ASPSOS-CFAR with $N = 16$, $L = 127$, $M = 3$ and noI = 0, 4. The corresponding mean acquisition time of each processor is also shown in Figure 27. It is observed from both figures that the S-CFAR has better performance than that

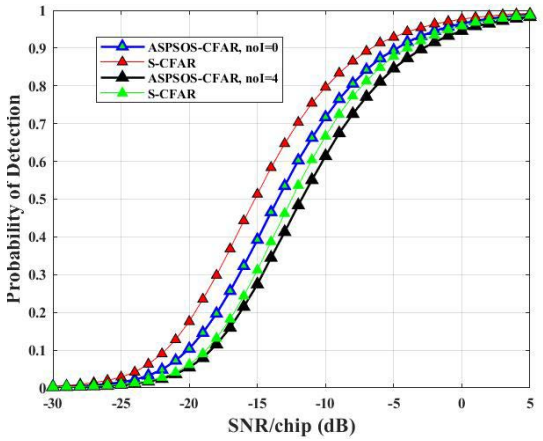

FIGURE 26. P_d versus SNR/chip in (dB) for S-CFAR and ASPSOS-CFAR algorithms when noI = 0, 4.

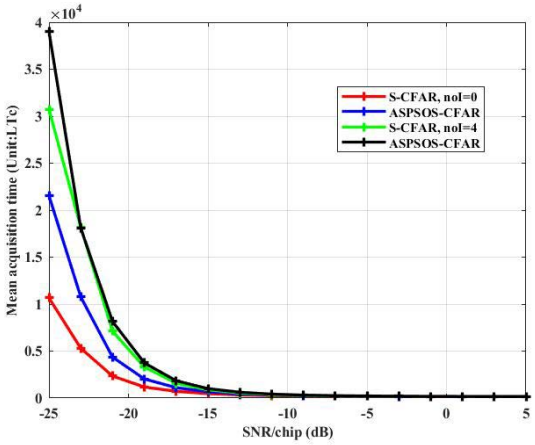

FIGURE 27. T_{acq} versus SNR/chip in (dB) for S-CFAR and ASPSOS-CFAR algorithms when noI = 0, 4.

of ASPSOS-CFAR. For the homogeneous environment, the difference in performance is quite pronounced because the ASPSOS-CFAR determines the number of interfering samples automatically with a tendency to overestimate the value of T_2; hence less reference window samples are involved in computing the adaptive decision threshold. However, for the non-homogeneous environment, there is a slight improvement in P_d for the S-CFAR over the ASPSOS-CFAR, especially for SNR/chip values in the range from -25 to 0 dB. Otherwise, the two processors have similar behaviour.

Next, we present comparisons for the S-CFAR with the set of processors of its class which exploit the cell under test to determine the adaptive threshold. Figures 28 and 29 show the probability of detection of PN acquisition system employing smart antennas and SOS-CFAR, GS-CFAR, and S-CFAR algorithms. The reference window size is set to $N = 16$, number of antennas $M = 3$, and correlation length $L = 127$, and number of interfering cells noI = 0,1,2,4. It is observed from Figure 28 that at $P_d = 0.8$ and noI = 0, the S-CFAR and GS-CFAR have 0.25 and 0.11 dB improvements in SNR/chip, respectively, compared to SOS-CFAR.

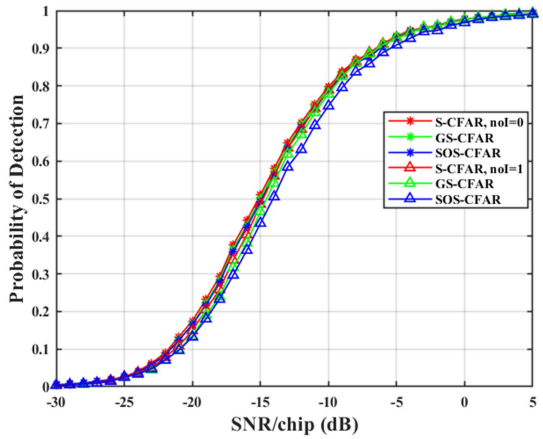

FIGURE 28. P_d versus SNR/chip in (dB) for S-CFAR, GS-CFAR and SOS-CFAR algorithms when noI = 0, 1.

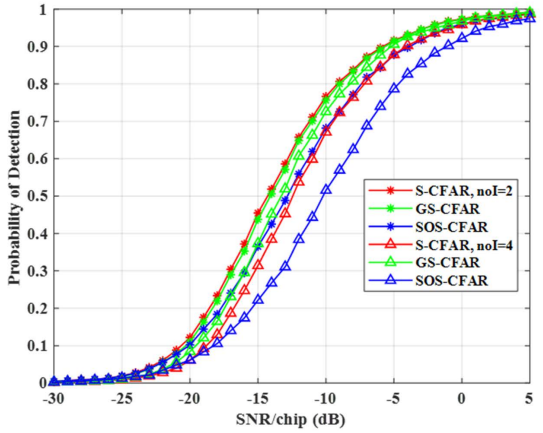

FIGURE 29. P_d versus SNR/chip in (dB) for S-CFAR, GS-CFAR and SOS-CFAR algorithms when noI = 2, 4.

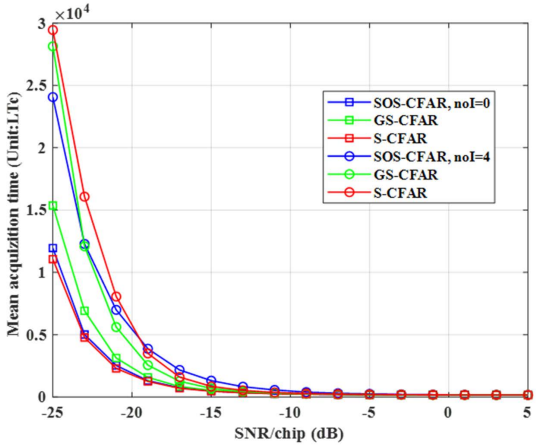

FIGURE 30. T_{acq} versus SNR/chip in (dB) for S-CFAR, GS-CFAR and SOS-CFAR algorithms.

However, this improvement decreases when the number of interfering cell reaches 4. In particular, the GS-CFAR has better performance in this case than that of S-CFAR and SOS-CFAR. At $P_d = 0.5$, the CFAR improvements of GS-CFAR

and S-CFAR are 3 and 2.2 dB, respectively, compared to the performance of SOS-CFAR. That is, GS-CFAR processor has more resistance to the effect of larger number of interfering samples than S-CFAR.

Figure 30 shows the corresponding T_{acq} for each processor when noI $= 0$ and 4. At noI $= 0$, the S-CFAR has better performance than both GS-CFAR and SOS-CFAR. But when noI $= 4$, the S-CFAR performance degrades compared to GS-CFAR. While SOS-CFAR is better than S-CFAR at low values of SNR/chip, S-CFAR shows better acquisition time at SNR/chip values above -19.5dB.

V. CONCLUSION

A DS-CDMA PN serial acquisition system using smart antenna and S-CFAR adaptive thresholding for wireless communication systems has been proposed and analyzed. The performance of proposed acquisition system has been evaluated in terms of three main metrics; P_{fa},P_d, and T_{acq}. Closed form expressions have been derived for P_{fa} and P_d. Numerical and simulation results have also been presented to investigate the effect of proposed PN acquisition scheme's parameters on the system performance. Several conclusions can be summarized from the conducted study, as follows:

- The probability of false alarm of proposed system does not depend on the observation interval or correlation length; and this conclusion is true regardless of the utilized number of antennas. Further, different values for S-CFAR processor's parameters may lead to the same value of probability of false alarm. Therefore, the user of S-CFAR processor should choose those parameters maximizing the probability of detection.
- The probability of detection increases and the mean acquisition time decreases as the number of antennas, reference window size, and correlation length increase. However, as the value of reference window size increases, the effect on the performance becomes less pronounced.
- The probability of detection and the mean acquisition time degrade as the number of interfering cells increases. However, the performance can be enhanced by using either larger number of antennas or longer observation interval.

The performance of proposed S-CFAR based PN acquisition system has been also compared with the class of processors relying solely on the reference window samples to define the adaptive threshold, and with the second class of processors exploiting both the reference window samples and the cell under test to determine appropriate threshold to maintain constant false alarm rate. For homogenous environment, the CA-CFAR processor has the optimum performance, while the S-CFAR processor has slight better performance than TM-CFAR, ASOS-CFAR and OS-CFAR processors. Further, the S-CFAR processor has better performance than the GS-CFAR and SOS-CFAR. For non-homogenous environment, the S-CFAR processor has better performance than TM-CFAR, OS-CFAR, and ASOS-CFAR processors when the number of interfering targets is relatively small. However, as the number of interfering targets increases, the TM-CFAR has better performance than S-CFAR at relatively small values of SNR/chip, and the two processors maintain almost the same performance at greater values of SNR/chip. Similarly, the S-CFAR processor performance becomes inferior to that of the GS-CFAR processor when the number of interfering targets increases, and in this case the GS-CFAR processor has better performance than that of S-CFAR and SOS-CFAR processors.

REFERENCES

[1] L. Xu, X. Yu, and T. A. Gulliver, "Intelligent outage probability prediction for mobile IoT networks based on an IGWO-Elman neural network," *IEEE Trans. Veh. Technol.*, vol. 70, no. 2, pp. 1365–1375, Feb. 2021.

[2] S. D. Ilcev, "Analyses of code division multiple access (CDMA) schemes for global mobile satellite communications (GMSC)," *TransNav, Int. J. Mar. Navigat. Saf. Sea Transp.*, vol. 14, no. 4, pp. 805–810, 2020.

[3] *Global Telecom Services Spending 2019*. Accessed: Apr. 16, 2021. [Online]. Available: https://www.statista.com/statistics/322995/worldwide-telecom-services-spending-forecast/

[4] I. W. Sandberg, J. T. Lo, C. L. Fancourt, J. C. Principe, S. Katagiri, and S. Haykin, *Nonlinear Dynamical Systems: Feedforward Neural Network Perspectives*, vol. 21. Hoboken, NJ, USA: Wiley, 2001.

[5] A. Polydoros and C. Weber, "A unified approach to serial search spread-spectrum code acquisition—Part I: General theory," *IEEE Trans. Commun.*, vol. COM-32, no. 5, pp. 542–549, May 1984.

[6] L.-L. Yang and L. Hanzo, "Serial acquisition of DS-CDMA signals in multipath fading mobile channels," *IEEE Trans. Veh. Technol.*, vol. 50, no. 2, pp. 617–628, Mar. 2001.

[7] E. A. Sourour and S. C. Gupta, "Direct-sequence spread-spectrum parallel acquisition in a fading mobile channel," *IEEE Trans. Commun.*, vol. 38, no. 7, pp. 992–998, Jul. 1990.

[8] W. Zhuang, "Noncoherent hybrid parallel PN code acquisition for CDMA mobile communications," *IEEE Trans. Veh. Technol.*, vol. 45, no. 4, pp. 643–656, Nov. 1996.

[9] R. Bekhakhecha and M. Barkat, "Simple PN synchronization using the OS-CFAR algorithm," in *Proc. Int. Workshop Adv. Control (IWAC)*, Guelma, Algeria, 2014, pp. 121–124.

[10] H. Puska, H. Saarnisaari, J. Iinatti, and P. Lilja, "Serial search code acquisition using smart antennas with single correlator or matched filter," *IEEE Trans. Commun.*, vol. 56, no. 2, pp. 299–308, Feb. 2008.

[11] H. Kwon, I. Song, S. Y. Kim, and S. Yoon, "Noncoherent constant false-alarm rate schemes with receive diversity for code acquisition under homogeneous and nonhomogeneous fading circumstances," *IEEE Trans. Veh. Technol.*, vol. 56, no. 4, pp. 2108–2120, Jul. 2007.

[12] C.-J. Kim, H.-J. Lee, and H.-S. Lee, "Adaptive acquisition of PN sequences for DSSS communications," *IEEE Trans. Commun.*, vol. 46, no. 8, pp. 993–996, Aug. 1998.

[13] M. Katz, J. Iinatti, and S. Glisic, "A comparative study of code acquisition using antenna diversity and beamforming techniques," in *Proc. IEEE 7th Int. Symp. Spread Spectr. Techn. Appl.*, vol. 1, Sep. 2002, pp. 223–227.

[14] H. Krouma, M. Barkat, K. Kemih, M. Benslama, and Y. Yacine, "Performance analysis of an adaptive threshold hybrid double-dwell system with antenna diversity for acquisition in DS-CDMA systems," *Int. J. Electron. Commun. Eng.*, vol. 2, no. 12, pp. 2782–2791, 2008.

[15] R. Bekhakhecha, M. Barkat, S. Alshebeili, and H. Tebbikh, "Adaptive acquisition of a PN code using OS-CFAR detection and antenna diversity for a multipath Rayleigh fading channel," in *Proc. Int. Conf. Comput. Commun. Eng.*, Kuala Lumpur, Malaysia, May 2006.

[16] R. Pickholtz, D. Schilling, and L. Milstein, "Theory of spread-spectrum communications—A tutorial," *IEEE Trans. Commun.*, vol. COM-30, no. 5, pp. 855–884, May 1982.

[17] C.-H. Lim, H.-S. Oh, D.-S. Han, and M.-J. Cho, "Adaptive hybrid acquisition with antenna diversity in CDMA systems," in *Proc. Commun. Netw.-Centric Oper., Creating Inf. Force (MILCOM)*, vol. 2, 2001, pp. 1243–1247.

[18] B. Wang and H. M. Kwon, "PN code acquisition using smart antenna for spread-spectrum wireless communications. I," *IEEE Trans. Veh. Technol.*, vol. 52, no. 1, pp. 142–149, Jan. 2003.

[19] A. El Zooghby, *Smart Antenna Engineering*. Morristown, NJ, USA: Artech, 2005.
[20] M. Barkat, *Signal Detection and Estimation*, 2nd ed. Norwood, MA, USA: Artech House, 2005.
[21] L. A. Addoweesh, "PN code acquisition using order statistics adaptive thresholding and smart antennas for DS/CDMA mobile communications in a multipath Rayleigh slowly fading channel," M.S. thesis, Dept. Comput. Eng., King Saud Univ., Riyadh, Saudi Arabia, 2014.
[22] N. Alhariqi, "PN acquisition using adaptive thresholding and smart antenna for direct sequence CDMA mobile communication," M.S. thesis, Dept. Comput. Eng., King Saud Univ., Riyadh, Saudi Arabia, 2013.
[23] A. Sofwan and M. Barkat, "PN code acquisition using smart antennas and adaptive thresholding trimmed-mean CFAR processing for CDMA communication," in *Proc. Spring Congr. Eng. Technol.*, Xi'an, China, May 2012, pp. 1–4.
[24] A. Jouini, A. Maali, M. Benssalah, A. Mesloub, G. Baudoin, and M. Hamadouche, "A robust auto-adaptive approach for serial acquisition of generalized multi-carrier spread spectrum in multipath fading mobile channels," *Int. J. Commun. Syst.*, vol. 34, no. 1, p. e4659, 2021.
[25] T.-T. Van Cao, "A CFAR thresholding approach based on test cell statistics," in *Proc. IEEE Radar Conf.*, Philadelphia, PA, USA, Apr. 2004, pp. 349–354.
[26] T. T. V. Cao, "Constant false-alarm rate algorithm based on test cell information," *IET Radar, Sonar Navigat.*, vol. 2, no. 3, pp. 200–213, Jun. 2008.
[27] M. I. Skolnik, *Introduction to Radar Systems*. New York, NY, USA: McGraw-Hill, 1982.
[28] A. Jalil, H. Yousaf, and M. I. Baig, "Analysis of CFAR techniques," in *Proc. 13th Int. Bhurban Conf. Appl. Sci. Technol. (IBCAST)*, Islamabad, Pakistan, Jan. 2016, pp. 654–659.
[29] E. W. Kang, *Radar System Analysis, Design, and Simulation*, 1st ed. Norwood, MA, USA: Artech House, 2008.
[30] P. P. Gandhi and S. A. Kassam, "Analysis of CFAR processors in non-homogeneous background," *IEEE Trans. Aerosp. Electron. Syst.*, vol. 24, no. 4, pp. 427–445, Jul. 1988.
[31] H. Rohling, "Radar CFAR thresholding in clutter and multiple target situations," *IEEE Trans. Aerosp. Electron. Syst.*, vol. AES-19, no. 4, pp. 608–621, Jul. 1983.
[32] J. Rickard and G. Dillard, "Adaptive detection algorithms for multiple-target situations," *IEEE Trans. Aerosp. Electron. Syst.*, vol. AES-13, no. 4, pp. 338–343, Jul. 1977.
[33] S. Erfanian and V. T. Vakili, "Introducing switching ordered statistic CFAR type I in different radar environments," *EURASIP J. Adv. Signal Process.*, vol. 2009, no. 1, pp. 1–11, Dec. 2009.
[34] L. Tabet and F. Soltani, "A generalized switching CFAR processor based on test cell statistics," *Signal, Image Video Process.*, vol. 3, no. 3, pp. 265–273, Sep. 2009.
[35] B. Sklar, *Digital Fundamentals and Applications*, 2nd ed. Englewood Cliffs, NJ, USA: Prentice-Hall, 2000.
[36] B. G. Lee and B.-H. Kim, *Scrambling Techniques for CDMA Communications*. New York, NY, USA: Springer, 2002.
[37] F. Gross, *Smart Antennas for Wireless Communications*. New York, NY, USA: McGraw-Hill, 2005.
[38] S. S. Haykin, *Adaptive Filter Theory*, 5th ed. London, U.K.: Pearson, 2013.

TAGHREED SAAD ALOFAISAN received the bachelor's degree in computer science from King Saud University, Riyadh, Saudi Arabia, where she is currently pursuing the master's degree with the Department of Computer Engineering, College of Computer and Information Sciences. She worked as a Computer Programmer at Imam Muhammed Bin Saud University. She is also working as a Computer Programmer at King Saud University. Her research interest includes signal detection in wireless communications. She is a member of the IEEE Computer Society.

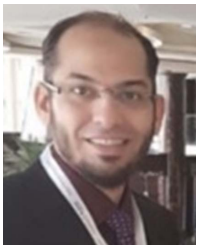

AMR M. RAGHEB received the B.S. (Hons.) and M.Sc. degrees in electrical engineering from Tanta University, Egypt, in 2001 and 2007, respectively, and the Ph.D. degree in electrical engineering from King Saud University, Riyadh, Saudi Arabia, in 2015. He was a Teaching Assistant (TA) with Tanta University, from 2003 to 2008. He was a TA with King Saud University, from 2010 to 2015. He has over seven years of experience with the Photonics Telecommunication Laboratory. He is currently an Assistant Professor with King Saud University. His current research interests include photonic-microwave integration, quantum dash-based lasers, free-space optical communication, optical modulation format identification, coherent optical receivers, multiformat high-speed optical transmitter, and passive optical networks.

AHMED B. IBRAHIM received the B.Sc. degree in computer science from Assuit University, Egypt, in 2007, and the Master of Biometrics in optics, image, vision and multimedia from the University of Paris-Est Créteil, France, in 2016. He is currently a Researcher at King Saud University. His research interests include machine learning, data analysis, and signal/image processing algorithms related to biometrics and biomedical signals.

MUSAED ALHUSSEIN was born in Riyadh, Saudi Arabia. He received the B.S. degree in computer engineering from King Saud University, Riyadh, in 1988, and the M.S. and Ph.D. degrees in computer science and engineering from the University of South Florida, Tampa, FL, USA, in 1992 and 1997, respectively. Since 1997, he has been with the Faculty of the Computer Engineering Department, College of Computer and Information Science, King Saud University. He is currently the Founder and the Director of the Embedded Computing and Signal Processing Research Laboratory. His research interests include typical topics of computer architecture and signal processing and with an emphasis on VLSI testing and verification, embedded and pervasive computing, cyber-physical systems, mobile cloud computing, big data, eHealthcare, and body area networks.

SALEH A. ALSHEBEILI was the Chairperson of the Electrical Engineering Department, King Saud University, from 2001 to 2005. He has over 27 years of teaching and research experience in the area of communications and signal processing. He was a member of the Board of Directors with the King Abdullah Institute for Research and Consulting Studies, from 2007 to 2009, and a member of the Board of Directors with the Prince Sultan Advanced Technologies Research Institute, from 2008 to 2017, where he was the Managing Director, from 2008 to 2011, and the Director of the Saudi-Telecom Research Chair, from 2008 to 2012. He has been the Director of the Technology Innovation Center, RF and Photonics in the e-Society, funded by the King Abdulaziz City for Science and Technology (KACST), since 2011. He is currently a Professor with the Electrical Engineering Department, King Saud University. He has also an active involvement in the review process of a number of research journals, KACST general directorate grants programs, and national and international symposiums and conferences. He has been on the Editorial Board of the *Journal of Engineering Sciences*, King Saud University, from 2009 to 2012.